

# Phase segregation on the nanoscale in $\text{Na}_2\text{C}_{60}$

G. Klupp,<sup>1,\*</sup> P. Matus,<sup>1</sup> D. Quintavalle,<sup>2,3</sup> L.F. Kiss,<sup>1</sup> É. Kováts,<sup>1</sup>  
N.M. Nemes,<sup>4</sup> K. Kamarás,<sup>1</sup> S. Pekker,<sup>1</sup> and A. Jánossy<sup>2,3</sup>

<sup>1</sup>*Research Institute for Solid State Physics and Optics,  
Hungarian Academy of Sciences, P.O. Box 49, Budapest, Hungary H-1525*

<sup>2</sup>*Institute of Physics, Budapest University of Technology and Economics, P.O. Box 91, Budapest, Hungary H-1521*

<sup>3</sup>*Solids in Magnetic Fields Research Group of the Hungarian Academy of Sciences, P.O. Box 91, Budapest, Hungary H-1521*

<sup>4</sup>*Instituto de Ciencia de Materiales de Madrid (CSIC), Cantoblanco, E-28049 Madrid, Spain*

(Dated: June 18, 2019)

$\text{Na}_2\text{C}_{60}$  is believed to be an electron-hole counterpart of the Mott-Jahn-Teller insulator  $\text{A}_4\text{C}_{60}$  salts. We present a study of infrared, ESR, NMR spectroscopy, X-ray diffraction, chemical composition and neutron scattering on this compound. Our spectroscopic results at room temperature can be reconciled in a picture of segregated, separate regions of the size 3–10 nm. We observe a significant insulating  $\text{C}_{60}$  phase and at least two more phases, one of which we assign to metallic  $\text{Na}_3\text{C}_{60}$ . The separation disappears on heating by jump diffusion of the sodium ions, which we followed by neutron scattering. Above  $\sim 460$  K we see infrared spectroscopic evidence of a Jahn-Teller distorted  $\text{C}_{60}^{2-}$  anion.

PACS numbers: 64.75.+g, 71.70.Ej, 61.48.+c, 71.20.Tx

## I. INTRODUCTION

The fullerene molecule,  $\text{C}_{60}$ , has three degenerate lowest unoccupied molecular orbitals (LUMO) and is a good electron acceptor that forms mono- through hexaanions relatively easily. The physical properties of the salts formed by the fulleride anions with alkali cations are in sharp contrast with a simplistic view of rigid-band filling. Solid  $\text{C}_{60}$  and  $\text{A}_6\text{C}_{60}$  (with  $\text{A}=\text{K}, \text{Rb}$ ) both have cubic structures and are non-magnetic band insulators with an empty and full band, respectively, derived from the LUMO orbitals.<sup>1</sup> A rigid-band model would suggest that all materials with partial filling (and the simplest possible cubic structure with one molecule per unit cell) must be either metals or magnetic Mott insulators.<sup>2</sup> However, this is not the case.  $\text{A}_3\text{C}_{60}$  salts have a half-filled band and are metals that are superconducting at low temperature,<sup>3</sup> but none of the other compositions have a metallic ground state. Although the low-temperature properties of cubic  $\text{AC}_{60}$  salts are difficult to establish ( $\text{C}_{60}^-$  ions polymerize below 400 K<sup>4,5</sup>), the magnetic susceptibility of the monomeric forms at high temperature is characteristic of paramagnetic Mott insulators.<sup>6</sup> The nonmagnetic insulators  $\text{A}_4\text{C}_{60}$  ( $\text{A} = \text{K}, \text{Rb}, \text{Cs}$ ) are the most thoroughly investigated series in this family. It was for these systems that the concept of the Mott-Jahn-Teller nonmagnetic insulator<sup>7</sup> has been put forward.

The argument combining Mott localization and Jahn-Teller effect can be summarized as follows. In order to minimize molecular energy,  $\text{C}_{60}^{n-}$  ions undergo Jahn-Teller distortion and subsequent splitting of the LUMO levels. The Jahn-Teller splitting is usually much smaller than the bandwidth in a conventional solid, but Mott localization can lead to band narrowing and singlet ground states for evenly charged ions. Singlet-triplet excitations in such a model correspond to a small spin gap ( $\approx 0.05$  eV),<sup>8</sup> whereas charge excitations from one

molecule to the next would cause a transport and optical gap of 0.5 eV.<sup>9</sup> The latter corresponds to the transition between Jahn-Teller split levels of  $t_{1u}$  origin, which would be optically forbidden on the same molecule.

Molecular calculations<sup>10</sup> show that the most significant Jahn-Teller distortion occurs for evenly charged ions  $\text{C}_{60}^{2-}$  and  $\text{C}_{60}^{4-}$  and involves elongation and flattening, respectively, along a three- or fivefold axis, leading to a fulleride ion with  $D_{3d}$  or  $D_{5d}$  point group. External fields, *e.g.* the Coulomb potential of the cations, can stabilize a distortion along a twofold axis, resulting in  $D_{2h}$  symmetry. This is the case in orthorhombic  $\text{Cs}_4\text{C}_{60}$ .<sup>11,12</sup> In  $\text{K}_4\text{C}_{60}$  and  $\text{Rb}_4\text{C}_{60}$  with average tetragonal structure<sup>13</sup> a frustration exists between molecular and crystal symmetry. In these salts, there is experimental evidence for a Mott-Jahn-Teller insulator ground state with low lying excited states<sup>8,9</sup> and the dominant role of molecular degrees of freedom over crystal field at higher temperatures in vibrational spectra.<sup>14,15</sup>

The electronic structure of  $\text{A}_2\text{C}_{60}$  salts is related to that of  $\text{A}_4\text{C}_{60}$  by electron-hole symmetry and thus they should also be insulators with the Jahn-Teller distortion in  $\text{C}_{60}^{2-}$  ions lifting the degeneracy. Direct comparison is hampered by the fact that of the  $\text{A}_2\text{C}_{60}$  family only  $\text{Na}_2\text{C}_{60}$  has been prepared so far, and its natural electron-hole counterpart,  $\text{Na}_4\text{C}_{60}$ , forms a polymer at room temperature.<sup>16</sup>  $\text{Na}_2\text{C}_{60}$ , nevertheless, is considered as an ideal material to test the role of Jahn-Teller distortions since in addition to the partial filling with even electrons it crystallizes in a face-centered cubic structure above 319 K,<sup>17,18</sup> where the threefold degeneracy of both  $t_{1u}$  LUMO's and  $T_{1u}$  vibrational transitions remains unchanged.  $\text{Na}_2\text{C}_{60}$  has indeed been investigated by several authors<sup>8,19,20</sup> but findings and interpretations by different groups have been contradictory. A detailed NMR (nuclear magnetic resonance) and ESR (electron spin resonance) study<sup>8</sup> interpreted the temper-

ature dependence of the spin susceptibility in the framework of a Mott–Jahn–Teller singlet ground state with low-energy triplet excitations. The authors concluded that the similar behavior of *bct*  $K_4C_{60}$  and simple cubic  $Na_2C_{60}$  proves the dominant role of molecular distortions over that of the environment. The spin-lattice relaxation at low temperature indicated that the band degeneracy is not completely lifted and the ground state might be weakly metallic. Kubozono *et al.*<sup>19</sup> interpret a sudden change at 50 K in the susceptibility and the Raman spectrum as a sign of a metal-insulator transition. Reference 20 reports hysteretic behavior in the ESR spectra in the temperature range of 300–400 K.

In this paper, we suggest that  $Na_2C_{60}$  is not a simple electron-hole analogue of  $C_{60}^{4-}$ , but it is yet another example of inhomogeneous charge distribution on the nanoscale. Spatial inhomogeneity is not uncommon in fulleride salts. Metastable cubic  $CsC_{60}$  seems to be a non-magnetic insulator with a charge disproportionation into  $C_{60}^{2-}$  ions and  $C_{60}$ .<sup>21,22</sup> Segregation of potassium ions into  $K_3C_{60}$  within a continuous  $C_{60}$  lattice has been observed for  $KC_{60}$ .<sup>23</sup> Disproportionation may also play a role in  $A_3C_{60}$ : a dynamic charge fluctuation of  $C_{60}^{3-}$  ions into  $C_{60}^{2-}$  and  $C_{60}^{4-}$  would stabilize the metallic character.<sup>24</sup>  $^{23}Na$  NMR and  $^{13}C$  magic-angle-spinning NMR data<sup>25</sup> in nominally  $Na_3C_{60}$  samples also suggest formation of distinct regions of fulleride ions with various charge states. In  $Na_2C_{60}$ , we present evidence from infrared (IR), ESR and NMR spectroscopy and neutron scattering that  $Na^+$  ions are inhomogeneously distributed on the scale of a few lattice constants within the ordered  $C_{60}$  lattice. This inhomogeneous distribution leads to at least two phases, one of which is  $C_{60}$  and one metallic  $Na_3C_{60}$ . The material appears homogeneous above  $\sim 460$  K where Na diffusion is fast.

Single phase alkali fulleride salts are difficult to prepare and differences in experimental findings often arise from variations in composition. However, for  $Na_2C_{60}$  most groups report the same X-ray diffraction pattern. A well-defined orientational transition is observed at 319 K;<sup>17,18</sup> at room temperature and below the  $C_{60}$  molecules are ordered in a  $Pa\bar{3}$  structure. The multiphase structure of  $Na_2C_{60}$  resolves the controversy between findings of different groups: this controversy stems more from the varying sensitivity of specific experimental methods to the presence of distinct phases than from variations in sample preparation.

## II. EXPERIMENTAL

$Na_2C_{60}$  was obtained by solid-state synthesis in inert gas atmosphere in a dry box. Stoichiometric amounts of Na metal and  $C_{60}$  powder were heated in a stainless steel capsule. The typical annealing sequence was first 23 days at 350 °C followed by 7 days at 450 °C. To homogenize the samples we reground them about once every five days. The progress of the reaction was moni-

tored by X-ray diffraction (XRD) and room-temperature infrared spectroscopy. After the final step, XRD results were identical to those in the literature.<sup>18</sup> Within the spatial resolution of XRD, a *single*  $Pa\bar{3}$  phase with a lattice constant of 14.18 Å was found. At this point we tested the high-temperature infrared spectrum as well, to prove that there is no residual  $C_{60}$  present. The samples were handled in inert atmosphere (He, Ar or vacuum) throughout all the following preparation and measurement procedures.

Infrared spectra were recorded on pressed KBr pellets in a Bruker IFS 28 FTIR instrument either in a cryostat under dynamic vacuum, or in argon atmosphere in a sealed sample holder with KBr windows, with 1 or 2  $cm^{-1}$  spectral resolution. Samples for investigation by XRD were enclosed in glass tubes and those for NMR, ESR and SQUID in quartz tubes.

The static susceptibility was measured by a Quantum Design MPMS-5S SQUID magnetometer between 5 and 600 K. We extracted the susceptibility from fixed-temperature magnetization data between 1 and 5 T. The low-field part was omitted in order to get rid of spurious ferromagnetic contributions.

High-frequency ESR spectra were measured on about 20 mg of  $Na_2C_{60}$  powder in a home-built spectrometer operating at 225 GHz (corresponding to a resonance magnetic field of 8.1 T). The 9 GHz spectrum was recorded with a commercial Bruker ELEXSYS 500 spectrometer.  $\alpha, \gamma$ -bis(diphenylene- $\beta$ -phenylallyl) (BDPA) was used as standard g-factor reference ( $g = 2.0025$ ).

NMR spectra were obtained by Fourier transformation of free induction decay (FID) signals. The FID signals were collected by a Tecmag Apollo HF spectrometer in 8.9 T static magnetic field (corresponding  $^{13}C$  frequency: 95 MHz). The frequency scales used are fractional frequency shifts  $\Delta f/f$  from the standard reference solution of tetramethylsilane (TMS) with positive shifts indicating higher resonant frequencies.

For neutron scattering measurements, 1.2 g of  $Na_2C_{60}$  powder was placed in an annular aluminum sample holder. Temperature-dependent elastic fixed-window scans (EFWS) were taken on both the sample and the empty sample container on the High Flux Backscattering Spectrometer of the NIST Center for Neutron Scattering.<sup>26</sup> The individual detector counts were normalized by the neutron monitor of the direct beam, binned into 5 K intervals to improve the signal-to-noise ratio and similar data from the empty sample container, with contributions of at most one third of the sample counts, were subtracted.

## III. RESULTS

We investigated the samples of nominal composition  $Na_2C_{60}$  by infrared, ESR and NMR spectroscopy, direct measurement of chemical composition and neutron scattering. First we summarize the limits of quantitative de-

termination using the methods we combine in this study. IR spectra yield the vibrational frequencies of individual fulleride anions, and reflect their charge and symmetry. While the intensity of a specific absorption peak assigned to a species (*e.g.* a molecular ion with a given charge) scales linearly with its concentration, the cross sections can differ considerably between species. In metallic systems, the free-electron background further complicates the spectra by smearing the vibrational peaks. ESR gives information on species with unpaired spins. The high-frequency resonances of various phases are well resolved and the relative spin susceptibilities can be determined. NMR intensities scale with the amount of the nucleus investigated, but in  $C_{60}$  anions, the position of the peaks does not shift enough with charge to be resolved.

Taking into account all the limitations and combining the information from individual methods, we conclude that none of the results at room temperature is compatible with the picture of a homogeneous material consisting of  $C_{60}^{2-}$  molecules. Below we describe the findings by individual methods in detail.

### A. Infrared spectroscopy

Figure 1 shows the IR spectra at 300 K and 480 K. A strong difference is observed in the range of the highest-frequency  $T_{1u}(4)$  mode, the most sensitive to the charge of  $C_{60}^{n-}$  anions. On cooling back from 480 K to room temperature, the original 300 K spectrum reappears after about two weeks.

We discuss first the high-temperature spectrum which is in accordance with the assumption of a homogeneous  $Na_2C_{60}$  phase and then the low-temperature phase which contradicts this assumption.

Of the four infrared active vibrations of  $C_{60}$ , the highest frequency  $T_{1u}$  mode is most sensitive to charge  $n$  when  $C_{60}^{n-}$  anions are formed. From the empirical linear relationship between the  $T_{1u}(4)$  frequency and  $n$ ,<sup>27</sup> we estimate the frequency in  $C_{60}^{2-}$  to be about  $1380\text{ cm}^{-1}$ , possibly with a splitting due to the molecular Jahn–Teller effect.<sup>14,28</sup> Indeed, above 460 K two bands are resolved at  $1369$  and  $1394\text{ cm}^{-1}$ , near the expected position of  $C_{60}^{2-}$ . The twofold splitting of the mode indicates  $D_{3d}$  or  $D_{5d}$  molecular symmetry, *i.e.* a Jahn–Teller distortion of *molecular* origin.<sup>10</sup>

The room-temperature spectrum (Fig. 1) shows a strong peak at  $1428\text{ cm}^{-1}$ , typical of neutral  $C_{60}$ , and a smeared one with a weak peak at  $1370\text{ cm}^{-1}$ . The spectrum does not change on cooling between 300 K and 80 K. The low-temperature spectra are in contradiction with expectations for a homogeneous  $Na_2C_{60}$  compound. The weak peak at  $1370\text{ cm}^{-1}$  is at the position expected for  $Na_3C_{60}$ .  $A_3C_{60}$  salts are metallic and show less intense vibrational peaks due to the large background from free-carrier absorption.<sup>27,29</sup>

The  $1428\text{ cm}^{-1}$  mode cannot be assigned to unreacted residual  $C_{60}$  since it disappears by heating above 460 K

and reappears on cooling back in a reproducible manner. The data rather suggest that the material contains a mixture of fulleride ions. We can positively identify neutral  $C_{60}$  molecules and  $C_{60}^{3-}$  ions at room temperature and below, and  $C_{60}^{2-}$  dianions at higher temperature. We cannot tell from the spectra whether the different vibrational signatures come from isolated sites embedded in some other matrix or from highly concentrated phases. However, from the metallic background it is probable that the phase containing  $C_{60}^{3-}$  is a metal, presumably  $Na_3C_{60}$ . We cannot exclude the presence of small amounts of other fulleride anions at low temperature, either; their vibrational peaks can be buried in the background around  $1400\text{ cm}^{-1}$ .

### B. Electron spin resonance and static susceptibility

The static susceptibility measured by SQUID magnetometry at 4 T shows three characteristic temperature ranges: i.)  $T < 100\text{ K}$ ; a Curie-like paramagnetic increase with decreasing temperature, ii.)  $100\text{ K} < T < 300\text{ K}$ ; an approximately constant susceptibility with  $\chi = 1.8 \cdot 10^{-7}\text{ emu/gOe}$ , and iii.)  $300\text{ K} < T < 600\text{ K}$ ; a continuous increase to about  $6 \cdot 10^{-7}\text{ emu/gOe}$ . The zero value of the static susceptibility is not corrected for core electron effects. The temperature-dependent part of the susceptibility measured by ESR at 9 GHz in Ref. 8 shows the same three characteristic ranges.

In the 225 GHz high-frequency ESR spectra, lines of three phases were resolved at all temperatures between 5 and 450 K. In a conventional spectrometer at 9 GHz, these lines were not resolved, a single line of 9 G peak-to-peak derivative linewidth was found at 300 K. A 225 GHz spectrum taken at 40 K is shown as an example in Fig. 2. We attribute the three lines to three different segregated phases in the nominally  $Na_2C_{60}$  material. The ESR line intensities are proportional to the spin susceptibilities of the various phases and are shown in Fig. 3. The full ESR spectra were decomposed into three Lorentzian lines and the fractional intensities for each line  $i$ ,  $I_i = \chi_i V_i / C$ , (the spin susceptibility,  $\chi_i$ , times the fractional volume,  $V_i$ ) were determined. The temperature dependence of the full ESR intensity,  $C = \Sigma I_i$ , was not measured directly, instead, we normalized the total ESR intensity data at each temperature to the static susceptibilities measured by SQUID.

At low temperature (Fig. 2), the static susceptibility is dominated by a single phase (Phase 1) with a Curie-like susceptibility corresponding to 1.3% of  $C_{60}^-$  (or other spin 1/2) free radicals with respect to the entire  $C_{60}$  content of the sample. We denote by Phase 2 the phase with the largest ESR intensity at ambient temperature. ESR of Phase 3 has a smaller g-factor than Phases 1 and 2 and could be followed in a wide temperature range despite the small intensity. Since the corresponding susceptibility does not vary strongly, it is possible that Phase 3 is metallic and may be assigned to the  $Na_3C_{60}$  observed by

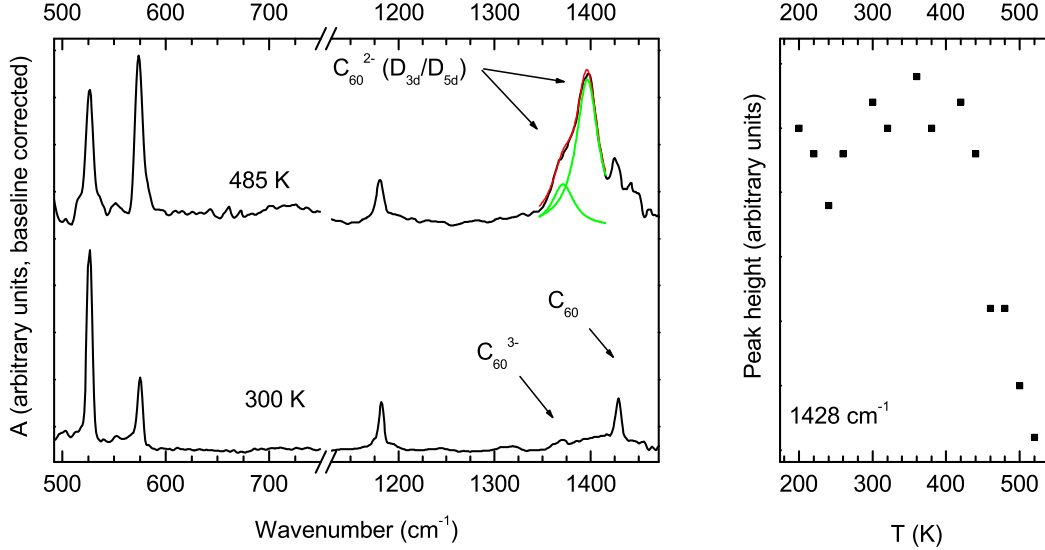


FIG. 1: (color online) Left panel: infrared absorption of  $\text{Na}_2\text{C}_{60}$  at 300 K and 485 K in the region of the principal  $\text{C}_{60}$  vibrations. Right panel: temperature dependence of the intensity of the  $1428\text{ cm}^{-1}$  line, characteristic of neutral  $\text{C}_{60}$ .

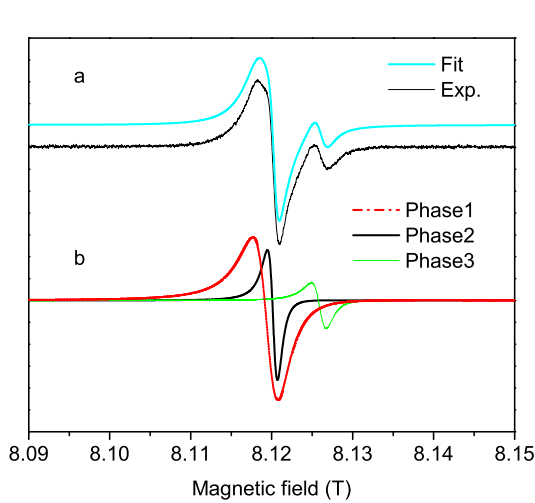


FIG. 2: (color online) Decomposition of 225 GHz ESR spectrum into lines corresponding to segregated phases at 40 K. a) experimental spectrum (black) and sum of three fitted lines (light blue) b) decomposition of experimental line into three segregated phases.

IR.

At about 450 K a structural transition takes place, the three low-temperature phases disappear and are replaced by a new phase (Fig. 4). This is the same temperature region where the  $1428\text{ cm}^{-1}$  IR line decreases. The single Lorentzian line indicates an increased homogeneity. The material is, however, still somewhat inhomogeneous between 450 and 500 K since spectra on heating and cooling are different. On rapid cooling (2.5 K/min) the sample

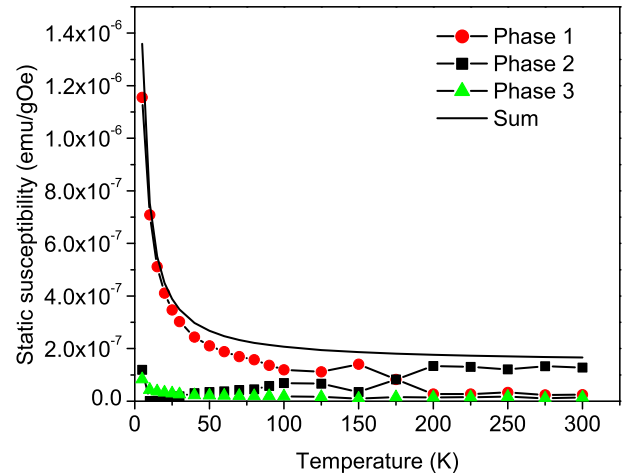


FIG. 3: (color online) Decomposition of static spin susceptibility into various phases from ESR. The absolute values of the susceptibility were determined from the static (SQUID) measurements.

is quenched into a homogeneous metastable state. The original phase-segregated material reappears after about two weeks at room temperature.

The main conclusion to be drawn from the ESR spectra is that in equilibrium the sample is inhomogeneous below 450 K.  $\text{C}_{60}$  paramagnetic ions with different g-factors due to differing environments will have a single ESR at an average g-factor if exchange interaction energies between them are larger than  $(\Delta g/g)\hbar\omega_L$  where  $\Delta g$  is the difference in g-factors and  $\omega_L$  is the Larmor frequency. Fulleride metals or semiconductors with lo-

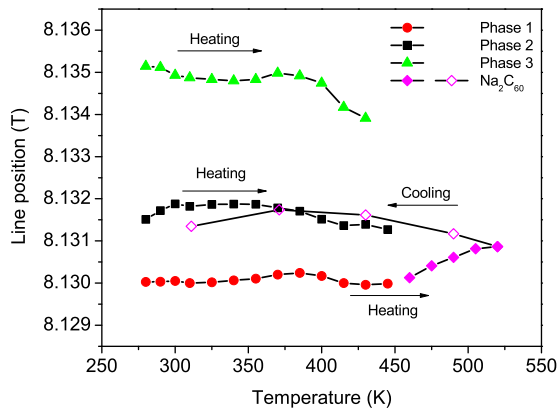


FIG. 4: (color online) Temperature dependence of 225 GHz ESR line positions of nominal  $\text{Na}_2\text{C}_{60}$  (g factor of Phase 1 at 300 K: 2.0012). Full (empty) symbols refer to heating (cooling). The three lines corresponding to various segregated phases merge into a single line on heating above 450 K indicating an increased homogeneity due to  $\text{Na}^+$  diffusion. On cooling to 300 K, a metastable phase is established that disappears after a few days.

calized  $\text{C}_{60}$  ions therefore exhibit a single line from the conduction and localized electrons. Neighboring paramagnetic  $\text{C}_{60}$  ions will not show separate resonances even if they are embedded in an insulator. Thus paramagnetic  $\text{C}_{60}$  ions in Phase 1 must be isolated from Phase 2 by nonmagnetic  $\text{C}_{60}$  ions. The simplest assignment is that Phase 1 is solid neutral  $\text{C}_{60}$  doped with a low concentration of isolated  $\text{Na}^+$  ions or small groups of  $\text{Na}^+$  ions. Phase 1 must be a non-negligible fraction of the material since it contains over 1% isolated free paramagnetic  $\text{C}_{60}$  ions surrounded by a shell of non-magnetic ions. We believe this phase is the neutral  $\text{C}_{60}$  phase detected by  $^{13}\text{C}$  NMR containing a small concentration of  $\text{Na}^+$  ions and ESR active  $\text{C}_{60}^-$ . A mixture of Phase 2 and Phase 3 appears to be the phase studied in detail by  $^{13}\text{C}$  and  $^{23}\text{Na}$  NMR and attributed to  $\text{Na}_2\text{C}_{60}$  by Brouet *et al.*<sup>8</sup> Above 450 K the  $\text{Na}^+$  ions diffuse rapidly in the crystal lattice and the sample becomes homogeneous.

### C. Nuclear magnetic resonance

Infrared absorption measurements detected  $\text{C}_{60}$  molecular ions with various charge states below 460 K and high-frequency ESR experiments revealed several phases in nominal  $\text{Na}_2\text{C}_{60}$ . The  $\text{C}_{60}$  concentration can be determined using NMR spectroscopy. Figure 5 shows the  $^{13}\text{C}$  NMR spectrum of a powder sample at 300 K. With conventional repetition rates of about  $1 \text{ s}^{-1}$  we observe a single NMR line around 178 ppm with chemical-shift anisotropy (shown in the lower panel of Fig. 5). This spectrum is very similar to that already published by Rachdi *et al.*<sup>30</sup> With a much longer repetition time (250 seconds), however, a further line appears at 143 ppm

(upper panel of Fig. 5), which we assign to neutral  $\text{C}_{60}$ .<sup>31</sup> As expected for pure  $\text{C}_{60}$ , the  $^{13}\text{C}$  spin-lattice relaxation time is long, about 50 seconds at 300 K. We used a repetition time more than five times the  $T_1$  spin-lattice relaxation time of this slowly relaxing spectral component to determine the spectral weights and estimate  $25 \pm 5\%$  neutral  $\text{C}_{60}$  content in the material. This high value is in agreement with the determination of chemical composition (see below).

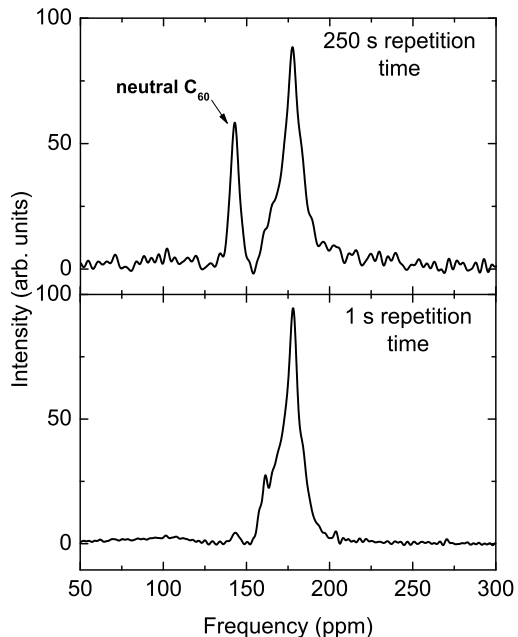


FIG. 5: NMR spectra at 300 K with two different repetition rates. At fast repetition rates only  $\text{C}_{60}^{n-}$  ions with short spin-lattice relaxation time are recorded. At slow repetition rates the spectrum of neutral  $\text{C}_{60}$  is also observed.

Unlike the three phases in high-frequency ESR spectra, only two are resolved by NMR. We assign these as neutral and charged  $\text{C}_{60}$ , respectively, where the charged part contains a mixture of phases, including both  $\text{Na}_3\text{C}_{60}$  and Phase 2. The  $^{13}\text{C}$  spin-lattice relaxation of charged  $\text{C}_{60}$  is many orders of magnitude faster than that of  $\text{C}_{60}$  ( $T_1$  roughly 100 ms compared to 100 s), because of the hyperfine interaction with conducting electrons. The large difference in relaxation rates indicates that cross-coupling between nuclei in the charged and neutral phases is small, so these nuclei must be well separated in space. More refined methods, *e.g.* MAS-NMR, would probably be able to resolve more phases.

### D. Chemical composition

In usual multiphase fulleride samples the simplest method to separate pristine  $\text{C}_{60}$  from its salts is extraction by toluene.<sup>32</sup> We extracted  $\text{C}_{60}$  from the nominally  $\text{Na}_2\text{C}_{60}$  material by soaking it in toluene for 11 days.

Following this treatment, we determined the  $C_{60}$  content of the solution by high-pressure liquid chromatography (HPLC). The weight percentage of  $C_{60}$  can be calculated from the concentration of the  $C_{60}$  solution and the weight of the starting material. To obtain the mole percentage of  $C_{60}$  we assume that the material contains only one  $Na_xC_{60}$  phase besides the  $C_{60}$  phase, but we do not assume that the total stoichiometry of the material is nominal  $Na_2C_{60}$ . If the Na-fulleride phase in the material were  $NaC_{60}$  then the  $C_{60}$  content would be 27 mole %. The other extreme,  $Na_{12}C_{60}$ , would give 33 mole %. This estimated composition of 27-33 %  $C_{60}$  is in reasonable agreement with the NMR results.

### E. Neutron scattering

Diffusion of sodium was directly observed using neutron scattering. In this measurement, the incident neutron energy is fixed at 2.08 meV and scattering processes are detected near the elastic line within the energy window of the resolution of the instrument (1  $\mu$ eV). Thus when a dynamic process, such as sodium jump diffusion, becomes faster than the corresponding timescale of 0.8 ns, the measured EFWS intensity decreases.<sup>33</sup> Figure 6 shows the temperature dependence of the elastic line at  $Q = 1 \text{ \AA}^{-1}$ . The intensity shows typical Debye-Waller type decrease overall, but an unusual drop appears around 400 K over approximately 20 K. Our interpretation is that the jump diffusion of sodium ions between tetrahedral and octahedral sites becomes fast enough above 400 K to be resolved by the instrument and thus the incoherent scattering contribution of the sodium ions is removed from the EFWS intensity. The EFWS intensity of the background is much smaller than that of  $Na_2C_{60}$  and its temperature dependence is featureless.

We can get an idea of the nature of the  $Na^+$  motion by looking at the  $Q$ -dependence of the anomalous drop of the EFWS, shown in the inset of Fig. 6. The detectors of the spectrometer integrate over  $0.2 \text{ \AA}^{-1}$  regions in  $Q$ . Diffraction peaks of  $Na_2C_{60}$ <sup>34</sup> between  $0.5 \text{ \AA}^{-1}$  and  $0.9 \text{ \AA}^{-1}$  and also between  $1.2 \text{ \AA}^{-1}$  and  $1.6 \text{ \AA}^{-1}$  obscure the EFWS, as indicated by empty circles, thus these points are less reliable. Nevertheless, the drop of the elastic intensity peaks near  $Q=1.1 \text{ \AA}^{-1}$ . In a jump-diffusion model, this corresponds to a jump distance of  $4.0 \pm 0.5 \text{ \AA}$ .<sup>35</sup>

Due to steric hindrance, the diffusion of  $Na^+$  ions can only proceed through the trigonal point between the tetrahedral and octahedral voids, *i.e.* in the  $\langle 111 \rangle$  direction. In this direction, removed  $4.0 \text{ \AA}$  from the tetrahedral site, there is an off-centered octahedral site. This site is special because it has the same nearest-neighbor distances as the tetrahedral site, so that the Coulomb interaction between the  $Na^+$  cation and the fulleride anions remains optimal. <sup>23</sup>Na NMR experiments by Schurko *et al.*<sup>25</sup> on samples with nominal composition  $Na_3C_{60}$ ,

indicating occupation of low-symmetry octahedral positions by  $Na^+$  ions, corroborate our results.

## IV. DISCUSSION

All the results presented above can be reconciled if we assume a synproportion/disproportion reaction



taking place on cooling after preparation from left to right and on heating from right to left. Combining the data, we can also draw quantitative conclusions as to the stoichiometry, the size of the domains, and the time scale of the dynamics.

ESR, infrared and NMR measurements all confirm the presence of neutral  $C_{60}$  in the material. While the former two methods yield qualitative results, NMR also provides quantitative data. From NMR and chemical composition studies, we obtain the range for the  $C_{60}$  content to be between 20 and 33 mole % at room temperature. We illustrate an idealized picture of the fully nanosegregated phases in Fig. 7, consisting of 33%  $C_{60}$  and 67%  $Na_3C_{60}$ . In reality at finite temperatures the reaction is probably not complete, partly because of entropy reasons and partly because the interfaces between the segregated regions must consist of fulleride ions only partially surrounded by sodium ions. These interfaces may be responsible for the additional ESR signal, the broad NMR line and the broad background of the IR spectrum between 1350 and 1440  $cm^{-1}$ .

The spectroscopic results apparently contradict the X-ray diffraction data which see the material as a single phase. We have to take into account, though, that while diffraction measures the average crystal structure, over a relatively large area, spectroscopy is sensitive to local structure, *i.e.* domains of a few molecules. X-ray diffraction averages out inhomogeneities less than about 100 Ångstroms, especially if the structure of the constituting phases is similar. In  $Na_3C_{60}$ , the fulleride ions occupy *fcc* sites identical to those of  $C_{60}$  molecules in a  $C_{60}$  crystal, and the lattice constant of  $Na_3C_{60}$  of 14.19 Å is very close to that of  $C_{60}$ , 14.15 Å.

The lower size limit of the homogeneous domains can be estimated from the metallic nature of the  $Na_3C_{60}$  phase. For metallic behavior, a thickness of a few molecules is required. The lattice constants are about 1.4 nm and the size of homogeneous domains has to be in the range of 3 to 10 nanometers.

At high temperature the nanosegregated phase changes into a homogeneous phase by sodium diffusion in a more or less unaltered  $C_{60}$  lattice. We observed in the neutron scattering experiments that sodium ions jump from site to site on the time scale of 0.8 ns at 400 K. In a nanosegregated structure with mobile sodium ions, diffusion leads to homogenization. The extra electrons migrate along with the ions because of Coulomb attraction, eventually leading to charge equilibrium in the system.

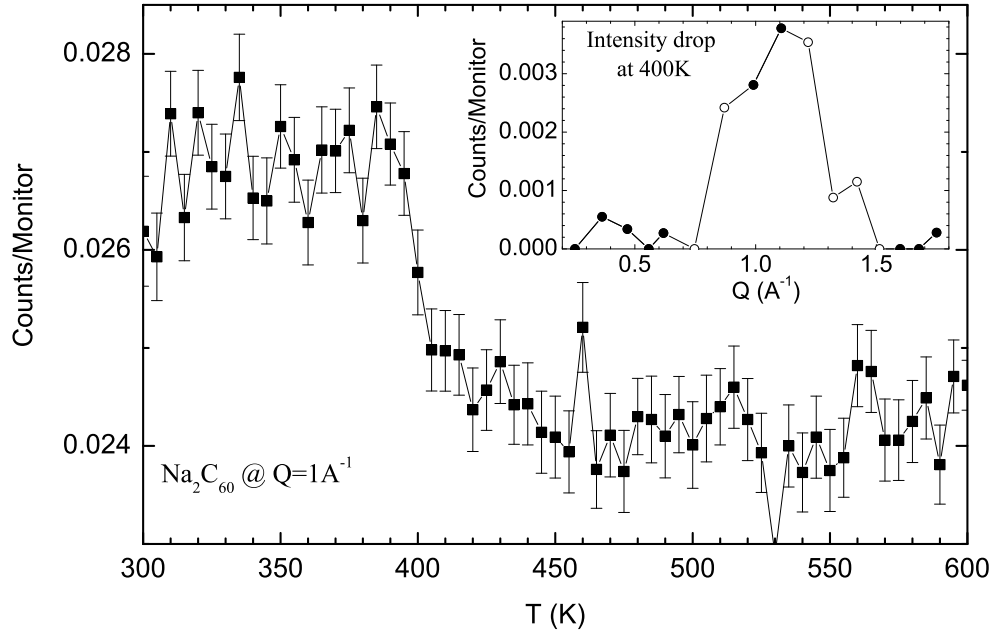


FIG. 6: Elastic fixed-window scan (EFWS) intensity of  $\text{Na}_2\text{C}_{60}$  at  $Q = 1 \text{ \AA}^{-1}$ . Inset:  $Q$ -dependence of the drop in EFWS intensity around 400 K (with empty circles indicating detectors obscured by  $\text{Na}_2\text{C}_{60}$  diffraction peaks).

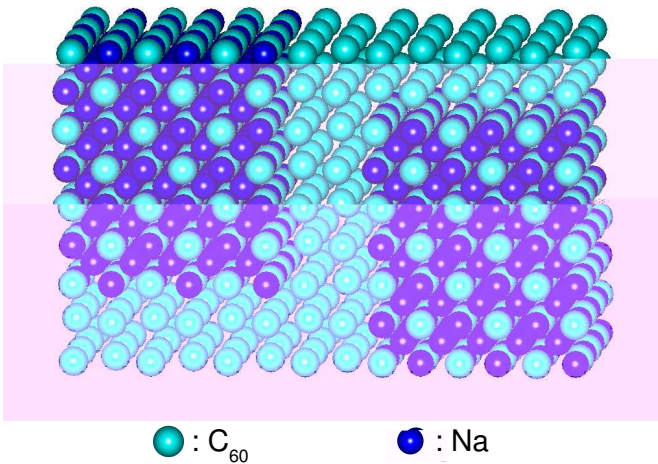


FIG. 7: (color online) Schematic view of segregated regions with and without sodium ions. Estimated area of the regions is between 3 and 10 nm.

Once the diffusion rate is high enough to achieve this equilibrium, the diffusion does not cause further charge migration and the material appears homogeneous by all spectroscopic methods. ESR shows a hysteretic phase segregation: on heating we observe segregated phases up to 450 K. Above 450 K there are no well separated conducting and insulating regions and the resonance is narrowed into a single line by electronic spin diffusion. This close-to-homogeneous phase is preserved for some time on cooling. A metastable phase with a single ESR line

is observed on cooling rapidly from 520 K to 300 K. Infrared spectra also show homogeneous charge distribution above 460 K, with indications of a metastable phase surviving on the time scale of weeks after cooling to room temperature.

The twofold splitting of the  $T_{1u}(4)$  infrared line at high temperature suggests that the symmetry of the molecules in the homogeneous phase is  $D_{3d}$  or  $D_{5d}$ . At first sight, this symmetry seems to contradict the cubic crystal structure, but can be explained as follows. Since in the high-temperature phase of  $\text{Na}_2\text{C}_{60}$  the molecules show quasifree rotation,<sup>17,18</sup> the distorting effect of the crystal field is averaged out. The absence of crystal field, however, does not mean that the shape of the molecule will stay spherical; it will be determined by the interaction of molecular vibrations with the two extra electrons occupying the LUMO (the molecular Jahn–Teller interaction).<sup>10</sup> In case of dianions, the result is a set of equivalent  $D_{3d}$  or  $D_{5d}$  distortions in different (symmetry-related) directions. These equivalent distortions transform into each other by a special motion called *pseudorotation*,<sup>10</sup> and their average will be icosahedral. (Tomita *et al.*<sup>36</sup> present a detailed explanation of the effect and provide experimental evidence from near-infrared spectroscopy of isolated  $\text{C}_{60}^-$  ions.) Nevertheless, if the time scale of a measurement is smaller than that of the pseudorotation, the distorted structure will be detected. This must be the case of the IR measurement. The high-temperature phase of  $\text{Na}_2\text{C}_{60}$  is another example of the dynamical Jahn–Teller effect in fulleride salts. The resulting symmetry strongly resembles

that occurring in the high-temperature phase of  $A_4C_{60}$  compounds,<sup>15</sup> proving the argument by Brouet *et al.* about the molecular interactions dominating over crystal field effects in both systems.<sup>8</sup>

## V. CONCLUSIONS

We have presented ample evidence from a wide range of analytical and spectroscopic methods that the fulleride salt with nominal composition  $Na_2C_{60}$  at room temperature forms nanosegregated domains with a large portion of  $C_{60}$  (containing  $Na^+$  ions in a low concentration) and other phases with high  $Na^+$  ion concentration, including metallic  $Na_3C_{60}$ . We estimate the amount of  $C_{60}$  in the material to be 20-33 % at 300 K. A synproportion reaction takes place on warming, homogeneity is achieved by the diffusion of sodium ions. In the homogeneous material, the  $C_{60}^{2-}$  anions undergo dynamic Jahn–Teller distortion to  $D_{3d}/D_{5d}$  symmetry.

Our samples showed the same X-ray diffraction pattern, 9 GHz ESR spectrum and low retention time NMR spectrum as those investigated previously. We expanded these experiments to different measuring condi-

tions and employed additional methods such as infrared spectroscopy, chemical composition determination and neutron scattering. All these experiments can be reconciled by assuming the nanosegregation model at low temperature and homogeneous  $Na_2C_{60}$  at high temperature. The results clarify the main reason for the contradictory results in the literature. They also underline the necessity of new experiments for the verification of the Mott–Jahn–Teller picture of insulating fulleride salts.

## Acknowledgments

We gratefully acknowledge the help of G. Oszlányi with X-ray diffraction measurements and extensive discussions. Work supported by the Hungarian National Research Fund under grant numbers OTKA T049338, T046700, TS049881 and T043255. This work utilized neutron research facilities of the National Institute of Standards and Technology, U.S. Department of Commerce, supported in part by the NSF DMR-0454672. N.N.M. is supported by the Juan de la Cierva fellowship of the Spanish Ministry of Education.

- 
- \* Electronic address: klupp@szfki.hu;  
URL: [www.szfki.hu/~klupp](http://www.szfki.hu/~klupp)
- <sup>1</sup> S. C. Erwin, in *Buckminsterfullerenes*, edited by W. A. Billups and M. Ciufolini (VCH, New York, 1992), p. 217.
  - <sup>2</sup> J. P. Lu, *Phys. Rev. B* **49**, 5687 (1994).
  - <sup>3</sup> A. F. Hebard, M. J. Rosseinsky, R. C. Haddon, D. W. Murphy, S. H. Glarum, T. T. M. Palstra, A. P. Ramirez, and A. R. Kortan, *Nature* **350**, 600 (1991).
  - <sup>4</sup> P. W. Stephens, G. Bortel, G. Faigel, M. Tegze, A. Jánossy, S. Pekker, G. Oszlányi, and L. Forró, *Nature* **370**, 636 (1994).
  - <sup>5</sup> S. Pekker, L. Forró, L. Mihály, and A. Jánossy, *Solid State Commun.* **90**, 349 (1994).
  - <sup>6</sup> F. Bommeli, L. Degiorgi, P. Wachter, Ö. Legeza, A. Jánossy, G. Oszlányi, O. Chauvet, and L. Forro, *Phys. Rev. B* **51**, 14794 (1995).
  - <sup>7</sup> M. Fabrizio and E. Tosatti, *Phys. Rev. B* **55**, 13465 (1997).
  - <sup>8</sup> V. Brouet, H. Alloul, S. Garaj, and L. Forró, *Phys. Rev. B* **66**, 155122 (2002).
  - <sup>9</sup> M. Knapfer and J. Fink, *Phys. Rev. Lett.* **79**, 2714 (1997).
  - <sup>10</sup> C. C. Chancey and M. C. M. O'Brien, *The Jahn-Teller Effect in  $C_{60}$  and Other Icosahedral Complexes* (Princeton University Press, Princeton, 1997).
  - <sup>11</sup> P. Dahlke, P. F. Henry, and M. J. Rosseinsky, *J. Mater. Chem.* **8**, 1571 (1998).
  - <sup>12</sup> P. Dahlke and M. J. Rosseinsky, *Chem. Mater.* **14**, 1285 (2002).
  - <sup>13</sup> C. A. Kuntscher, G. M. Bendele, and P. W. Stephens, *Phys. Rev. B* **55**, R3366 (1997).
  - <sup>14</sup> K. Kamarás, G. Klupp, D. B. Tanner, A. F. Hebard, N. M. Nemes, and J. E. Fischer, *Phys. Rev. B* **65**, 052103 (2002).
  - <sup>15</sup> G. Klupp, K. Kamarás, N. M. Nemes, C. M. Brown, and J. Leão, *Phys. Rev. B* **73**, 085415 (2006).
  - <sup>16</sup> G. Oszlányi, G. Baumgartner, G. Faigel, and L. Forró, *Phys. Rev. Lett.* **78**, 4438 (1997).
  - <sup>17</sup> T. Yildirim, J. E. Fischer, P. W. Stephens, and A. R. McGhie, in *Progress in Fullerene Research*, edited by H. Kuzmany, J. Fink, M. Mehring, and S. Roth (World Scientific, Singapore, 1994), p. 235.
  - <sup>18</sup> T. Yildirim, J. E. Fischer, A. B. Harris, P. W. Stephens, D. Liu, L. Brard, R. M. Strongin, and A. B. Smith, III, *Phys. Rev. Lett.* **71**, 1383 (1993).
  - <sup>19</sup> Y. Kubozono, Y. Takabayashi, S. Fujiki, S. Kashino, T. Kambe, Y. Iwasa, and S. Emura, *Phys. Rev. B* **59**, 15062 (1999).
  - <sup>20</sup> P. Petit, J. Robert, J.-J. André, and J. E. Fischer, in *Progress in Fullerene Research*, edited by H. Kuzmany, J. Fink, M. Mehring, and S. Roth (World Scientific, 1994), p. 478.
  - <sup>21</sup> V. Brouet, H. Alloul, F. Quéré, G. Baumgartner, and L. Forró, *Phys. Rev. Lett.* **82**, 2131 (1999).
  - <sup>22</sup> V. Brouet, H. Alloul, and L. Forró, *Phys. Rev. B* **66**, 155123 (2002).
  - <sup>23</sup> G. Faigel, G. Bortel, M. Tegze, L. Granasy, S. Pekker, G. Oszlányi, O. Chauvet, G. Baumgartner, L. Forro, P. W. Stephens, G. Mihaly, and A. Janossy, *Phys. Rev. B* **52**, 3199 (1995).
  - <sup>24</sup> V. Brouet, H. Alloul, T.-N. Le, S. Garaj, and L. Forró, *Phys. Rev. Lett.* **86**, 4680 (2001).
  - <sup>25</sup> R. W. Schurko, M. J. Willans, B. Skadtchenko, and D. M. Antonelli, *J. Solid State Chem.* **177**, 2255 (2004).
  - <sup>26</sup> A. Meyer, R. M. Dimeo, P. M. Gehring, and D. A. Neumann, *Rev. Sci. Instrum.* **74**, 2759 (2003).
  - <sup>27</sup> T. Pichler, R. Winkler, and H. Kuzmany, *Phys. Rev. B* **49**, 15879 (1994).
  - <sup>28</sup> V. C. Long, J. L. Musfeldt, K. Kamarás, A. Schilder, and

- W. Schütz, Phys. Rev. B **58**, 14338 (1998).
- <sup>29</sup> M. C. Martin, X. Du, J. Kwon, and L. Mihaly, Phys. Rev. B **47**, 14607 (1993).
- <sup>30</sup> F. Rachdi, L. Hajji, M. Galtier, T. Yildirim, J. E. Fischer, C. Goze, and M. Mehring, Phys. Rev. B **56**, 7831 (1997).
- <sup>31</sup> R. Tycko, G. Dabbagh, R. M. Fleming, R. C. Haddon, A. V. Makhija, and S. M. Zahurak, Phys. Rev. Lett. **67**, 1886 (1991).
- <sup>32</sup> M. Carrard, L. Forro, L. Mihaly, and S. Pekker, Synth. Met. **80**, 29 (1996).
- <sup>33</sup> T. Becker and J. C. Smith, Phys. Rev. E **67**, 021904 (2003).
- <sup>34</sup> M. J. Rosseinsky, D. W. Murphy, R. M. Fleming, R. Tycko, A. P. Ramirez, T. Siegrist, G. Dabbagh, and S. E. Barrett, Nature **356**, 416 (1992).
- <sup>35</sup> J. DeWall, R. M. Dimeo, and P. E. Sokol, J. Low Temp. Phys. **129**, 171 (2002).
- <sup>36</sup> S. Tomita, J. U. Andersen, E. Bonderup, P. Hvelplund, B. Liu, S. B. Nielsen, U. V. Pedersen, J. Rangama, K. Hansen, and O. Echt, Phys. Rev. Lett. **94**, 053002 (2005).